Solid State Science and Technology, Vol. 32, No. 2 (2024) 106-111
https://doi.org/10.66514/ssst32-2-106-111

Thermal Decomposition, Phase Formation and Microstructure Analysis of Carbon Nanotubes Assisted Sol-Gel Derived $La_{0.6}Sr_{0.4}CoO_{3-\delta}$ Material

Abdullah Abdul Samat[1,2,], Siti Hajar Zahari[1], Murizam Darus[1,3], Nafisah Osman[4]*

[1]Faculty of Mechanical Engineering and Technology, Universiti Malaysia Perlis Pauh Putra Campus, 02600 Arau, Perlis, Malaysia

[2]Centre of Excellence Unmanned Aerial Systems (COEUAS), Universiti Malaysia Perlis, 01000 Kangar, Perlis, Malaysia

[3]Centre of Excellence Geopolymer and Green Technology (CEGeoGTech) Universiti Malaysia Perlis, 01000 Kangar, Perlis, Malaysia

[4]Faculty of Applied Sciences, Universiti Teknologi MARA, 02600 Arau, Perlis Malaysia

** Corresponding author; email: abdullahabdul@unimap.edu.my*

Received: 26 August 2024 / Accepted: 14 November 2024

ABSTRACT

In the present work, $La_{0.6}Sr_{0.4}CoO_{3-\delta}$ (LSC) material is prepared with the aid of carbon nanotubes (CNTs) as dispersant and is characterized by thermal gravimetric analyzer (TGA), X-ray diffractometer (XRD), scanning electron microscope/energy dispersive X-ray (SEM/EDX) spectrometer and BET instrument. Decomposition of unwanted materials in the as-synthesized powder were completed at 600 °C and single LSC perovskite phase was formed at 900 °C. The calcined powder with surface area of 1.95 m^2/g and agglomeration index of 33.71 is made up of homogeneous with almost identical shape of particles. All elements of the single LSC perovskite phase are close to their nominal mole fraction.

Keywords: Agglomeration; calcination; ceramics; LSC; nanomaterial; perovskite

INTRODUCTION

Perovskite-type oxide materials with ABO_3 formula are extensively being used in protonic ceramic fuel cell (PCFC) application as electrolyte and electrode components due to their excellent and interesting properties such electrical conductivity, catalytic activity, dielectric, ferroelectric, piezoelectric and pyroelectric behaviors. The A-site is normally a rare earth element such as strontium, barium, and lanthanum while B-site is normally a transition element such as cobalt, cerium, zirconium, iron, and yttrium. One of the perovskite-type oxide materials which has been developed for PCFC as cathode component is lanthanum strontium cobaltite, $La_{0.6}Sr_{0.4}CoO_{3-\delta}$ (LSC)

material [1–3]. An excellent candidate of cathode material for PCFC application should has the following properties: (i) mixed ionic-electronic conductor; (ii) good catalytic activity; (iii) adequate porosity ranging between 20% – 40%; (iv) almost similar coefficient of thermal expansion with other components (electrolyte and interconnect); (v) stable under oxidizing environment and (vi) polarization resistance less than 1 Ω cm^2 [4,5]. Generally, all of the aforementioned properties depend on the cathode materials powder properties such as microstructure and purity. The microstructure and purity of a powder material are well known to be influenced by the processing techniques employed to produce the powder.

Various techniques were developed to produce perovskite-type oxide materials including LSC material. One of the common methods is the sol-gel method. It is popular due to its ability to produce ultrafine or nanosized powder at low processing temperature. Furthermore, a well-known drawback of this method is formation of hard agglomerated particles, reducing surface area of the produced powder and affecting overall electrochemical performance of an SOFC or a PCFC cell. Therefore, modifying the sol-gel method by employing promising chemical agent is an approach to overcome or minimize the drawback. One of the promising chemical agents is dispersing agents such as carbon black [6], activated carbon [7] and carbon nanotubes (CNTs) [8].

An attempt has been made to produce LSC material by using activated carbon as dispersing agent as reported in our previous work [9]. The produced powder still forms agglomerated particles with agglomeration index of 5.33. To further improve the properties of the produced LSC powder, CNTs was suggested to replace the activated carbon since there are very limited works that report on the powder properties of perovskite-type oxide materials prepared through sol-gel method using CNTs as dispersing agent, particularly the LSC material. Thus, this work will serve as a first and preliminary report on thermal decomposition behavior, phase structure formation and microstructure properties of CNTs assisted sol-gel derived LSC powder material.

MATERIALS AND METHODS

Powder material of $La_{0.6}Sr_{0.4}CoO_{3-\delta}$ (LSC) was produced via carbon nanotubes (CNTs) assisted sol-gel method with the aid of carbon nanotubes (CNTs). High purity (ACROS, >99%) precursor materials of $La(NO_3)_3$, $Sr(NO_3)_2$ and $Co(NO_3)_2$ were dissolved in 150 mL deionized water to produce a solution of metal nitrate salt by stirring process on a hotplate with stirrer for an hour. After all of the precursor materials were fully dissolved, citric acid (MERCK, 99.5%) and ethylenediaminetetraacetic acid (99%, ACROS) were added. Then, the pH value of the solution was adjusted to be 0.5. Next, ethylene glycol (ACROS, 99.95%) was introduced into the solution and followed by adding an amount of CNTs (Sigma Aldrich, >95% carbon basis). To form a viscous gel, the solution was slowly heated from 100 °C up to 200 °C for several hours. The obtained gel was subjected to drying process at 250 °C for 24 h, forming a coarse sponge-like structure. It was then grounded in an agate mortar and calcined at different temperatures for 5 h.

Thermal decomposition characteristic of the dried and grounded coarse sponge-like structure was analyzed on a thermal gravimetric analyzer, TGA (STA6000, Perkin Elmer, USA). For the calcined powder, its phase structure identification and formation were analyzed on an X-ray diffractometer, XRD (XRD6000, Shimadzu, Japan) with the aid of a software (PANalytical X'Pert HighScore Plus version 4.5). The calcined powder morphology and elemental

composition of the calcined powder was analyzed on a scanning electron microscope, SEM (Carl Zeiss SMT Supra-40VP, Germany) and energy dispersive X-ray, EDX (EVO MA 10, Germany) spectrometer. Surface area of the calcined powder was analyzed by BET surface area and porosity analyzer (Micromeritic ASAP 2020, USA).

RESULTS AND DISCUSSION

Thermal decomposition of the dried and grounded coarse sponge-like structure

A typical thermogravimetric curve for the grounded coarse sponge-like structure powder after dried at 250 °C is shown in Figure 1. It can be seen that thermal decomposition of the dried coarse powder occurred in multiple stages. There are at least three weight loss stages and the weight loss percentage at each stage is presented and briefly explained in Table 1. From the table, a complete decomposition of unwanted materials in the dried coarse powder was achieved at 600 °C with a total weight loss of 89.53%. Based on the thermal decomposition analysis result, the dried coarse powder was proposed to be calcined at temperatures higher than 600 °C to produce a single LSC perovskite phase.

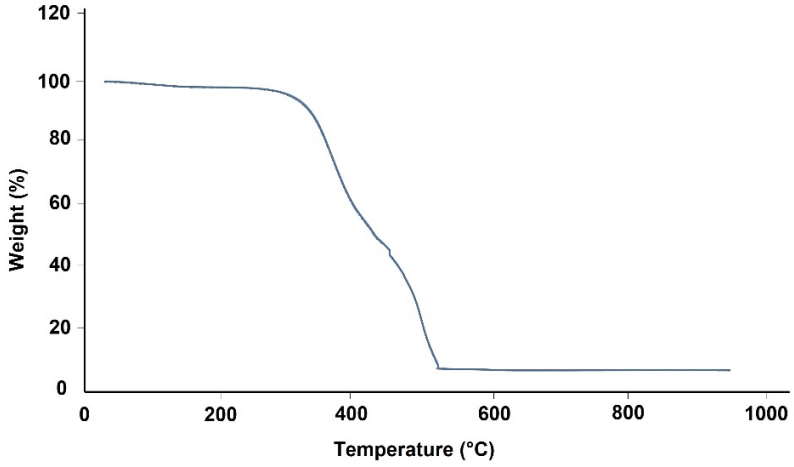

Figure 1. Thermal gravimetric curve for the coarse powder after dried at 250 °C

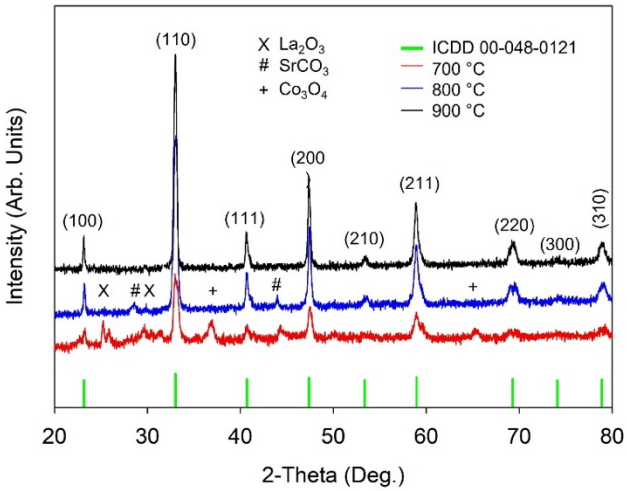

Figure 2. Patterns of powder X-ray diffraction for the powders calcined at 700 °C, 800 °C and 900 °C for 5 h

Table 1. Weight loss percentage at each stage for the coarse powder after dried at 250 °C and its description

Temperature range (°C)	Stage	Weight loss (%)	Description
30 – 180	1	2.54	• Dehydration of water and adsorbed moisture • Decomposition of leftover unwanted compounds with low boiling point (B_p) Nitrate compounds (B_p = 160 °C) Citric acid (B_p = 175 °C) Ethylene glycol (B_p = 197 °C)
181 – 520	2	89.53	• Decomposition high B_p compounds such as ethylenediaminetetraacetic acid and CNTs
521 – 600	3	0.96	• Decomposition of trapped carbonaceous residue formed after decomposition of compounds at stage 2 • Desired oxide compound (LSC material) is expected starting to form at this stage

Table 1. LSC perovskite phase percentage in the calcined powders

Calcination temperature (°C)	LSC perovskite phase percentage (%)	Secondary phase
700	69.78	La_2O_3, $SrCO_3$ and Co_3O_4
800	92.15	La_2O_3 and $SrCO_3$
900	100.00	-

Phase formation and identification of the calcined powder

Patterns of powder X-ray diffraction (PXRD) for the dried powders after calcined at 700 °C, 800 °C and 900 °C for the 2θ ranging from 20° to 80° are presented in Figure 2. The strongest peaks in all PXRD patterns were complemented to reference code 00-048-0121 of the International Centre for Diffraction Data (ICDD) with cubic structure and Pm-3m space group. The strongest peaks were respectively indexed to their Miller indices (hkl) of (100), (110), (200), (210), (211), (220), (300) and (310). Several peaks belong to the impurity phases such as strontium carbonate ($SrCO_3$), cobalt oxide (Co_3O_4) and lanthanum oxide (La_2O_3) were also present in the PXRD patterns. However, as the calcination temperature rose from 700 °C to 800 °C, intensity of the impurity peaks declined. Percentage of perovskite and/or secondary phases formed in each of the calcined powder is shown in Table 2. A single LSC perovskite phase prepared through the CNTs-assisted sol-gel method in this work was formed at 900 °C. The result is consistent with our previous works [9,10]. In addition, the result also agreed with the thermal decomposition analysis result which mentioned that the single LSC perovskite phase may form at temperature higher than 600 °C.

Morphology and elemental distribution of the calcined powder

Figure 3 shows the typical morphology of single ABO_3 perovskite phase powder. The image was captured at magnification of ×5000 using secondary electron mode. The powder consists of almost identical shape and homogeneous particles. The particles formed a network structure by connecting to each other. The measured value of BET surface area for the powder is 1.95 m^2/g. The value is lower than the single LSC perovskite phase derived from activated carbon assisted sol-gel method in our previous work (9.87 m^2/g) [9]. The low BET surface area value might be affected by high agglomeration index value which is 33.71. The value of agglomeration index reflects the dispersibility and gives an estimation of the average number of primary particles in the agglomerates of the produced powder [11]. To further reduce the value, the amount of CNTs added during the synthesis process will be further optimized. All elements (La, Sr, and Co) in the produced single LSC perovskite phase powder is equally distributed since their experimental mole fraction are close to their nominal mole fraction as shown in Table 3.

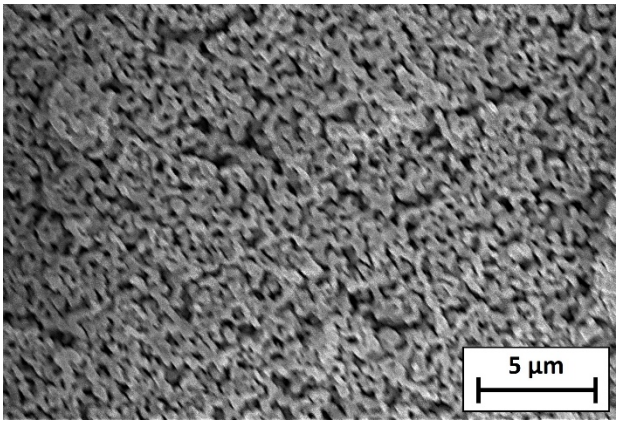

Figure 3. Morphology of the carbon nanotubes assisted sol-gel derived LSC powder after calcined at 900 °C

Table 2. Elemental composition of cobalt (Co), strontium (Sr) and lanthanum (La) in the carbon nanotubes assisted sol-gel derived LSC powder after calcined at 900 °C

Element	Actual mole fraction (mol)	Experimental mole fraction (mol)
Co	1.00	1.00 ± 0.00
Sr	0.40	0.37 ± 0.02
La	0.60	0.58 ± 0.07

CONCLUSIONS

A single $La_{0.6}Sr_{0.4}CoO_{3-\delta}$ (LSC) perovskite material was successfully produced through the sol-gel method assisted with carbon nanotubes (CNTs) as dispersant. The thermal decomposition characteristic of the dried powder was completed at 600 °C with three stages of weight loss. The powders calcined at 700 °C and 800 °C formed a mixture of LSC perovskite phase and secondary phases (La_2O_3, $SrCO_3$ and Co_3O_4) while the powder calcined at 900 °C formed a pure or single LSC perovskite phase. The single LSC perovskite phase has identical particles with surface area of with surface area of 1.95 m^2/g and agglomeration index of 33.71. Experimental mole

fractions of La, Sr and Co elements were close to their nominal mole fractions. Further works on optimizing CNTs amount in producing better qualities and properties of LSC single perovskite phase are in progress and the outcomes will be presented elsewhere.

ACKNOWLEDGMENTS

This work is fully funded by the Fundamental Research Grant Scheme (FRGS/1/2020/STG05/UNIMAP/02/10) provided by the Ministry of Higher Education of Malaysia. The authors would also like to thank Universiti Malaysia Perlis and Universiti Teknologi MARA (Perlis Branch) for providing supports and facilities.

REFERENCES

[1] H.A. Ishfaq, M.Z. Han, M.T. Mehran, R. Raza, W.H. Tanveer, S. Bibi, A. Hussain, H. A. Muhammad, R.H. Song (2021). Boosting performance of the solid oxide fuel cell by facile nano-tailoring of $La_{0.6}Sr_{0.4}CoO_{3-\delta}$ cathode, *Int. J. Hydrog. Energy* **47**(88)**,** 37587.

[2] Z. Huang, Z. Liu, H. Hu, J. Wang, M. Chen, B. Cao, Q. Wang, J. Yang, W. Guan, T. Liang (2022). Evaluation of $La_{0.6}Sr_{0.4}CoO_{3-\delta}$-$Ce_{0.85}Sm_{0.075}Nd_{0.075}O_{2-\delta}$ composite cathodes for intermediate temperature solid oxide fuel cells, *Ceram. Int.* **48**, 16319.

[3] C. Kim, H. Lee, I. Jang, S. Kim, H. Yoon, U. Paik, T. Song (2021). Subcontinuous 2D $La_{0.6}Sr_{0.4}CoO_{3-\delta}$ nanosheet as an efficient charge conductor for boosting the cathodic activity of solid oxide fuel cells, *Electrochimica Acta* **366**, 137371.

[4] N.N.M. Tahirm, N.A. Baharuddin, A.A. Samat, N. Osman, M.R. Somalu (2022). A review on cathode materials for conventional and proton-conducting solid oxide fuel cells, *J. Alloys Compd.* **894**, 162458.

[5] C. Sun, R. Hui, J. Roller (2010). Cathode materials for solid oxide fuel cells: a review, *J. Solid State Electrochem.* **14**, 1125.

[6] J.H. Kim,Y.M. Park, H. Kim (2011). Nano-structured cathodes based on $La_{0.6}Sr_{0.4}Co_{0.2}Fe_{0.8}O_{3-\delta}$ for solid oxide fuel cells, *J. Power Sources* **196**, 3544.

[7] I. Ismail, N. Osman, A.M.M. Jani (2020). $La_{0.6}Sr_{0.4}Co_{0.2}Fe_{0.8}O_{3-\delta}$ powder: a simple microstructure modification strategy for enhanced cathode electrochemical performance, *J. Sol-Gel Sci. Technol.* **94**, 435.

[8] N.I.A. Malek, I. Ismail, A.M.M. Jani, N. Osman (2020). Characterization of $LaSrCoFeO_3$ cathode material prepared with the aid of functionalized carbon nanotubes for proton conducting fuel cell, *AIP Conf. Proc.* **2221**, 030001.

[9] A. Abdul Samat. A.A. Jais. M.R. Somalu, N. Osman N, A. Muchtar, K.L. Lim (2018). Electrical and electrochemical characteristics of $La_{0.6}Sr_{0.4}CoO_{3-\delta}$ cathode materials synthesized by a modified citrate-EDTA sol-gel method assisted with activated carbon for proton-conducting solid oxide fuel cell application, *J. Sol-Gel Sci. Technol.* **86**, 617.

[10] A. Abdul Samat, M.R. Somalu, A. Muchtar. O.H. Hassan, N. Osman (2016). LSC cathode prepared by polymeric complexation method for proton-conducting SOFC application, *J. Sol-Gel Sci. Technol.* **78**, 382.

[11] M. Anwar, A.S.A. Muhammed, A.M. Abdalla, R.M. Somalu, A. Muchtar (2017). Effect of sintering temperature on the microstructure and ionic conductivity of $Ce_{0.8}Sm_{0.1}Ba_{0.1}O_{2-\delta}$ electrolyte, *Process. Appl. Ceram.* **11**, 67.